Trajectory Dynamics Study of Collision-Induced Dissociation of the Ar + CH₄ Reaction at Hyperthermal Conditions: Vibrational Excitation and Isotope Substitution

J. M. C. Marques,*,† E. Martínez-Núñez,‡ and S. A. Vázquez‡

Departamento de Química, Universidade de Coimbra, 3004-535 Coimbra, Portugal, and Departamento de Química Física, Universidad de Santiago de Compostela, Santiago de Compostela E-15782, Spain

Received: February 24, 2006; In Final Form: March 29, 2006

We investigate the role of vibrational energy excitation of methane and two deuterated species (CD_4 and CH_2D_2) in the collision-induced dissociation (CID) process with argon at hyperthermal energies. The quasi-classical trajectory method has been applied, and the reactive Ar + CH_4 system has been modeled by using a modified version of the CH_4 potential energy surface of Duchovic et al. (*J. Phys. Chem.* **1984**, *88*, 1339) and the Ar−CH_4 intermolecular potential function obtained by Troya (*J. Phys. Chem. A* **2005**, *109*, 5814). This study clearly shows that CID is markedly enhanced with vibrational excitation and, to a lesser degree, with collision energy. In general, CID increases by exciting stretch vibrational modes of the reactant molecule. For the direct dissociation of CH_4, however, the CID cross sections appear to be essentially independent of which vibrational mode is initially excited. In all situations studied, the CID cross sections are always greater for the Ar + CD_4 reaction than for the Ar + CH_4 one, the Ar + CH_2D_2 being an intermediate situation. A detailed analysis of the energy transfer processes, including their relation with CID, is also presented.

1. Introduction

Collision-induced dissociation (CID) phenomena have been always related to the study of microscopic dynamics of the energy transfer (ET) among all degrees of freedom of the involved species. Although many possibilities may arise, a typical CID study implies the activation of a molecular species by a rare gas atom, followed by its dissociation into two or more fragments. Most of ET studies have been devoted to understanding the mechanisms of ET occurring between translational and internal degrees of freedom during the collision process and the exchange of vibrational and rotational energy arising in the intramolecular dynamics and unimolecular dissociation processes. Significant activity was directed at characterizing the mechanisms whereby highly internally excited molecules lose energy to a bath of nonreactive species through collisional ET.[1,2]

From a theoretical point of view, the quasi-classical trajectory (QCT) method has played a fundamental role to acquire a qualitative (and sometimes quantitative) interpretation of CID and ET phenomena at the molecular level.[3–6] In particular, the QCT method has shown to be reliable in the study of energy transfer occurring in highly excited molecules.[7,8] Moreover, it is well-known that quite often the QCT method is the only way to study processes taking place under conditions that are extremely hard to simulate experimentally. Among these, we point out the chemistry occurring in flames, as well as the reactions in the high atmosphere and in the interstellar media. In addition, the simulation of the low-earth orbit (LEO) environment is recognized to be very important in anticipating problems related to the degradation of materials used to coat the spacecrafts operating at such altitudes (i.e., from 100 to 700

km). LEO conditions are characterized by very low pressure, extreme variations of temperature, ultraviolet radiation, and the existence of several chemical species (especially, atomic oxygen) that may collide with spacecrafts at high velocities (∼8 km s⁻¹) causing important damage to polymer-based materials of their coat.[9] In recent years, both the Schatz group and the Minton group have been very active in studying CID and ET processes at LEO conditions; specifically, their attention has been focused on the hyperthermal collisional dynamics of O (³P) with hydrocarbons,[10–13] N_2 and Ar with hydrocarbon polymers,[14,15] and Ar with ethane.[16] Schatz and collaborators applied the direct dynamics version of the QCT method in which the energy and its gradients are calculated "on-the-fly" as the trajectory is integrated, while the experiments at Minton's laboratory have been performed with the use of a crossed molecular beams apparatus that incorporates a fast-atom beam source.[17–19]

The Ar + CH_4 collisional system has been the subject of various theoretical[20–26] and experimental[27–32] studies concerning both CID and ET processes. The main goal of most of these studies has been the determination of dissociation rate coefficients in the high-temperature regime, which is considered to be important for the CH_4/O_2 combustion chemistry.[33] Particularly, we have performed[25] the first QCT study of the title reaction where the rate coefficient has been calculated in the temperature range 2500 ≤ *T*/K ≤ 4500; general agreement between experimental[30] and our theoretical[25] rate coefficients has been achieved after adequate correction of the CH_3 zero-point energy (ZPE), as calculated by using the corresponding normal-mode harmonic frequencies. In addition, we have also used the QCT method to obtain[25] energy-transfer parameters from which the $\langle \Delta E \rangle$ (the average energy transferred in all collisions) and $\langle \Delta E^2 \rangle^{1/2}$ (the root-mean-squared energy transferred in all collisions) values show good agreement with values deduced[24] from experiment,[30] while overestimating them in the case of $\langle \Delta E_d \rangle$ (the average energy transferred in deactivating collisions).

* To whom correspondence should be addressed. E-mail: qtmarque@ci.uc.pt.
† Universidade de Coimbra.
‡ Universidade de Santiago de Compostela.

TABLE 1: Fundamental Frequencies and Zero-Point Energy (ZPE) of Reactants CH$_4$, CD$_4$, and CH$_2$D$_2$ and Products CH$_3$, CD$_3$, CH$_2$D, and CHD$_2$ Arising in the Potential Energy Surface[25,43] Used in This Work

| system | vibrational mode frequencies[a] (cm^{-1}) | | | | ZPE (eV) |
	ν_1	ν_2	ν_3	ν_4	
CH$_4$	1423 (3)	1608 (2)	3084 (1)	3266 (3)	1.263
CD$_4$	1080 (3)	1137 (2)	2181 (1)	2408 (3)	0.925
CH$_2$D$_2$	1104 (1), 1182 (1), 1343 (1)	1393 (1), 1523 (1)	2284 (1)	2409 (1), 3185 (1), 3263 (1)	1.096
CH$_3$	394 (1)	1471 (2)	3039 (1)	3208 (2)	0.793
CD$_3$	306 (1)	1080 (2)	2149 (1)	2395 (2)	0.583
CH$_2$D	367 (1)	1231 (1), 1464 (1)	2304(1)	3106 (1), 3208 (1)	0.724
CHD$_2$	338 (1)	1087 (1), 1346 (1)	2222 (1)	2396 (1), 3161 (1)	0.654

^{a} The degeneracy of each mode is given in parentheses. Although CH$_2$D$_2$ has nine nondegenerated modes, they are still grouped in four sets associated to the symbols ν_1 (bend-type modes), ν_2 (bend-type modes), ν_3 (symmetric-stretch-type mode), and ν_4 (antisymmetric-stretch-type modes) (see the text).

Recently, Troya[26] has applied the QCT direct-dynamics approach by using quantum-mechanical semiempirical Hamiltonians to investigate the role of Ar + CH$_4$ and Ar + CF$_4$ hyperthermal collisions in the erosion of hydrogenated and fluorinated hydrocarbon polymers in LEO atmosphere. This dynamics study[26] has shown that collisions of hyperthermal argon atoms with methane in its ground vibrational state leads to low values of the CID cross sections even at high relative translational energies (e.g., 10 eV). Additionally, CID and collisional ET to internal modes of the alkane molecule is enhanced by fluorination, which has been attributed[26] to both the decrease in the hydrocarbon vibrational frequencies and an increase of the steepness of the corresponding intermolecular potential. Since Troya has considered that the initial vibrational energies of both CH$_4$ and CF$_4$ molecules were thermalized at T = 300 K, it is impossible to envisage the influence of vibrational excitation on CID and ET. Indeed, it is expected that collisions occurring between the gases at orbital altitude may have sufficient energy to excite infrared-active molecules to various vibrational states.[34] Moreover, Varandas and collaborators[35-41] have suggested that local thermodynamic disequilibrium (LTD) conditions may play an important role in the chemistry of atmosphere, providing a clue for explaining the "ozone-deficit problem" and "HO$_x$ dilemma".[39,41] More than a half century ago, Meinel[42] associated near-infrared night-time air-glow in the mesopause with LTD conditions because of the vibrational excited OH ($^2\Pi$) radicals formed from the H + O$_3$ reaction.

In the present work, we have studied the dynamics of hyperthermal argon species with highly internally excited CH$_4$, CD$_4$, and CH$_2$D$_2$ molecules. We endeavor to elucidate whether vibrational excitation may contribute to the erosion of hydrocarbon polymers in LEO hyperthermal conditions. A second goal of this trajectory study is the assessment of vibrational-mode specificity and deuteration effects in CID and ET. The plan of the paper is as follows: In section 2 we describe the trajectory calculation, while the main results are presented and discussed in section 3. Some conclusions are gathered in section 4.

2. Trajectory Calculations

In the present dynamics study, we have applied an improved version[25] of the CH$_4$ potential energy surface of Duchovic et al.,[43] which proved[25] to be more reliable than the original one,[43] to reproduce the vibrational excitation of methane. In addition, the intermolecular Ar−CH$_4$ interactions have been modeled by a pairwise generalized exponential function whose parameters have been obtained by a fit to CCSD(T)/cc-pVTZ ab initio points.[26] This intermolecular potential accurately describes the ab initio data[26] up to energies of ~10 eV, while the range of applicability of the one[44] used in our previous work[25] extends

only up to ~5 eV. Since both intramolecular[43,25] and intermolecular[26] potential functions have been extensively described in the original papers, no further details are given here.

To investigate the importance of isotope substitution in the title reaction, we have carried out trajectory calculations for Ar + CH$_4$, Ar + CD$_4$, and Ar + CH$_2$D$_2$ by using an adapted version[45-47] of the MERCURY code,[48] which allows the identification of all possible reactive channels.[45] Note that, for Ar + CH$_2$D$_2$, one may obtain both CH$_2$D and CHD$_2$ products, while for Ar + CH$_4$ and Ar + CD$_4$ only one type of products arises (i.e., CH$_3$ and CD$_3$, respectively). Batches of 40 000 trajectories have been run for each set of initial conditions, and the integration of the Hamilton equations of motion has been done by a combined fourth-order Runge−Kutta and sixth-order Adams−Moulton predictor−corrector algorithm with a time-step of 0.01 fs, which ensured good energy conservation. The reactants are initially separated by 14 Å and the integration is halted when argon and, in the case of dissociation, one hydrogen (or deuterium) become separated from the polyatomic molecule by more than 15 Å. The maximum impact parameter b_{max} has been optimized by applying the method of Lim and Gilbert,[49] which consists of the calculation of the second moment of the energy-transfer ($\langle \Delta E^2 \rangle$) whose converged value arises from the summation of all the contributions from trajectories falling in the equally spaced subsets of the interval [0, b_{max}]; as in our previous work,[25] the convergence is attained when the contribution to $\langle \Delta E^2 \rangle$ from adding an extra impact parameter subset becomes less than 2×10^{-2} cm^{-2}, which was chosen to reflect the effect of energy transfer in inelastic collisions.

For the three isotopomers of methane, we have studied the influence on the title reaction of (i) increasing collision energy, (ii) vibrational energy content, and (iii) specific vibrational-mode excitation. The rotational energy attributed to each axis of inertia was always $RT/2$ (R is the gas constant), with T fixed at 300 K. Concerning i, we have run trajectories for E_{tr} = 5, 6, 8, and 10 eV, while 4.757 eV of vibrational energy was assigned to the normal modes according to a microcanonical distribution,[50] so that the internal energy content always coincides with the classical threshold for dissociation of methane (i.e., 110.6 kcal mol^{-1} ≈ 4.796 eV). To study the influence of ii and iii on the CID process, five additional batches were run for a fixed collision energy of 8 eV. In one of these, we have reduced by $^1/_2$ (i.e., to 2.3785 eV) the energy distributed microcanonically among the vibrational modes. In the other four batches, a total of 4.757 eV was distributed among the vibrational degrees of freedom in order to excite one of the sets of modes labeled as ν_i (i = 1−4) in Table 1 (degenerate modes for CH$_4$ and CD$_4$) at each time, while the remaining have only their zero-point energy. Of course, in the case of CH$_2$D$_2$ the vibrational modes become nondegenerate for symmetry reasons, but it is still

Dissociation of the Ar + CH$_4$ Reaction

J. Phys. Chem. A, Vol. 110, No. 22, 2006 **7115**

TABLE 2: Results of the Trajectory Calculations for the Ar + CH$_4$ Reaction

E_{tr} (eV)	E_{vib} (eV)	type of vibrational excitation	b_{max} (Å)	$N_{CH_3}{}^a$	$N_{CH_4^*}{}^b$	$\sigma_{CID} \pm \Delta\sigma_{CID}{}^c$ (Å^2)
5	4.757	microcanonical	5.5	31	1560	0.074 ± 0.013 (3.780 ± 0.093)
6	4.757	microcanonical	5.5	61	2074	0.145 ± 0.018 (5.072 ± 0.107)
8	2.3785	microcanonical	5.0	4	29	0.008 ± 0.004 (0.065 ± 0.011)
	4.757	microcanonical	5.5	178	3185	0.423 ± 0.032 (7.990 ± 0.132)
		ν_1	5.5	175	3049	0.416 ± 0.031 (7.660 ± 0.129)
		ν_2	5.6	168	2994	0.414 ± 0.032 (7.788 ± 0.133)
		ν_3	5.5	137	3458	0.325 ± 0.028 (8.541 ± 0.136)
		ν_4	5.5	145	3535	0.344 ± 0.028 (8.743 ± 0.137)
10	4.757	microcanonical	5.4	345	4049	0.790 ± 0.042 (10.063 ± 0.143)

^{a} Number of trajectories leading to direct dissociation. ^{b} Number of trajectories leading to formation of CH$_4$ complexes that may dissociate to form products with the corresponding ZPE. ^{c} Direct-mechanism CID cross sections and the corresponding Monte Carlo standard deviations: values in parentheses are the total CID cross sections, including the contributions from both N_{CH_3} and $N_{CH_4^*}$ (see the text).

TABLE 3: Results of the Trajectory Calculations for the Ar + CD$_4$ Reaction

E_{tr} (eV)	E_{vib} (eV)	type of vibrational excitation	b_{max} (Å)	$N_{CD_3}{}^a$	$N_{CD_4^*}{}^b$	$\sigma_{CID} \pm \Delta\sigma_{CID}{}^c$ (Å^2)
5	4.757	microcanonical	5.5	77	3575	0.183 ± 0.021 (8.676 ± 0.137)
6	4.757	microcanonical	5.5	145	4155	0.344 ± 0.028 (10.216 ± 0.147)
8	2.3785	microcanonical	5.0	34	279	0.067 ± 0.011 (0.614 ± 0.035)
	4.757	microcanonical	5.5	369	4914	0.877 ± 0.045 (12.552 ± 0.161)
		ν_1	5.5	374	4773	0.888 ± 0.046 (12.228 ± 0.159)
		ν_2	5.8	308	4141	0.814 ± 0.046 (11.755 ± 0.166)
		ν_3	5.5	601	4978	1.428 ± 0.058 (13.255 ± 0.165)
		ν_4	5.5	430	5278	1.022 ± 0.049 (13.561 ± 0.166)
10	4.757	microcanonical	5.4	682	5407	1.562 ± 0.059 (13.946 ± 0.164)

^{a} Number of trajectories leading to direct dissociation. ^{b} Number of trajectories leading to formation of CD$_4$ complexes that may dissociate to form products with the corresponding ZPE. ^{c} Direct-mechanism CID cross sections and the corresponding Monte Carlo standard deviations; values in parentheses are the total CID cross sections, including the contributions from both N_{CD_3} and $N_{CD_4^*}$ (see the text).

possible to group the modes in four sets (still designated as ν_1, ν_2, ν_3, and ν_4) according to the similarity of their vibrational motion[51] and then excite each of them. The amount of vibrational energy assigned to each mode was proportional to its ZPE.

In the final analysis, we have considered as reactive those trajectories in which the internal energy of the product species is above the ZPE calculated by using the normal-mode harmonic frequencies of CH$_3$, whose values are given in Table 1. Similarly, the formation of excited species CH$_4^*$, CD$_4^*$, and CH$_2$D$_2^*$ follow the same criterion, that is, only trajectories where the internal energy content of the excited complex is sufficient to form products with the corresponding ZPE are considered in the statistical analysis. Although the quantum mechanical requirement for ZPE is in general associated with the vibrational energy content rather than with the internal one, the reason for applying the latter here as ZPE criterium relies on our previous observation that this leads to Ar + CH$_4$ rate constants in better agreement with experiment.[25] Because CH$_2$D$_2^*$ may lead to either CHD$_2$ or CH$_2$D, we used Rice−Ramsperg−Kassel−Marcus (RRKM) theory to estimate the branching ratio of both products.

3. Results and Discussion

The numerical results of the present trajectory calculations are shown in Tables 2, 3, and 4 for Ar + CH$_4$, Ar + CD$_4$, and Ar + CH$_2$D$_2$, respectively. The analysis of these results focus on two main topics: collision-induced dissociation (CID) and energy transfer. A discussion about the importance of isotope substitution and reactants vibrational energization is also given.

3.1. CID. The collision-induced dissociation (CID) of vibrationally excited methane may follow essentially one of two mechanisms: (i) direct or (ii) indirect dissociation. In the first case, the abstraction of one hydrogen (or deuterium) atom from

methane is a direct result of the interaction with the hyperthermal argon, which leads to immediate dissociation. Conversely, the second mechanism implies the formation of an excited methane complex, owing to the energy transferred from relative translation to the internal degrees of freedom, and which may last for many periods of rotation before dissociation can occur. In fact, trajectories lasting for more than 9000 ps have been observed in our previous work on Ar + CH$_4$.[25] Rigorously, trajectories following mechanism ii should be continued in order to verify whether they dissociate or not. However, since such a procedure is very time-consuming and hence impractical, we have adopted the alternative approach of considering as reactive trajectories all of those resulting in complexes with internal energy above the ZPE of products. Of course, this constitutes an upper-bound to the value of the indirect-type dissociation. For Ar + CH$_4$ and Ar + CD$_4$, the total CID cross sections, which include the contributions from both direct and indirect dissociation, are given in parentheses in Tables 2 and 3, respectively; the corresponding values for Ar + CH$_2$D$_2$ are shown in the last column of Table 4.

Moreover, we have displayed in Figure 1a the CID cross sections obtained from indirect dissociation for the three systems; in the case of Ar + CH$_2$D$_2$, we have represented separately the CID cross sections for formation of CHD$_2$ and CH$_2$D. It is clear from this figure and Table 4 that the formation of CHD$_2$ is favored over CH$_2$D, which may be attributed to the difference in the corresponding zero-point energies [E_{ZPE}(CH$_2$D) > E_{ZPE}(CHD$_2$)]. In this comparison, the contributions from both CH$_2$D and CHD$_2$ must be added to get the total cross section for CH$_2$D$_2^*$. In addition, the CID via indirect dissociation increases as the deuteration of methane increases. This is an expected result since the internal energy of the arising complexes has to fulfill the ZPE requirements of the corresponding product molecules, and E_{ZPE}(CH$_3$) > E_{ZPE}(CH$_2$D) > E_{ZPE}(CHD$_2$) >

TABLE 4: Results of the Trajectory Calculations for the Ar + CH₂D₂ Reaction

E_{tr} (eV)	E_{vib} (eV)	type of vibrational excitation	b_{max} (Å)	$N_{CH_2D_2^*}{}^a$	CH₂D formation[b]			CHD₂ formation[c]			$\sigma_{CID} \pm \Delta\sigma_{CID}{}^d$ (Å²)
					N_d	N_{RRKM}	$\sigma_d \pm \Delta\sigma_d$ (Å²)	N_d	N_{RRKM}	$\sigma_d \pm \Delta\sigma_d$ (Å²)	
5	4.757	microcanonical	5.8	2516	26	639	0.069 ± 0.013	22	1877	0.058 ± 0.012	6.774 ± 0.129
6	4.757	microcanonical	5.5	3422	43	958	0.102 ± 0.016	48	2464	0.114 ± 0.016	8.346 ± 0.134
8	2.3785	microcanonical	5.0	152	11	42	0.022 ± 0.006	7	110	0.014 ± 0.005	0.334 ± 0.026
	4.757	microcanonical	5.5	4247	162	1270	0.385 ± 0.030	124	2977	0.295 ± 0.026	12.830 ± 0.172
		ν_1	5.8	3853	146	1158	0.386 ± 0.032	82	2695	0.217 ± 0.024	10.782 ± 0.160
		ν_2	5.6	3756	103	1112	0.254 ± 0.025	104	2644	0.275 ± 0.027	9.761 ± 0.147
		ν_3	5.5	4473	614	1340	1.459 ± 0.058	27	3133	0.064 ± 0.012	12.150 ± 0.159
		ν_4	5.5	4652	54	1391	0.128 ± 0.017	238	3261	0.565 ± 0.036	11.746 ± 0.156
10	4.757	microcanonical	5.8	4413	247	1389	0.653 ± 0.041	196	3024	0.518 ± 0.037	12.830 ± 0.172

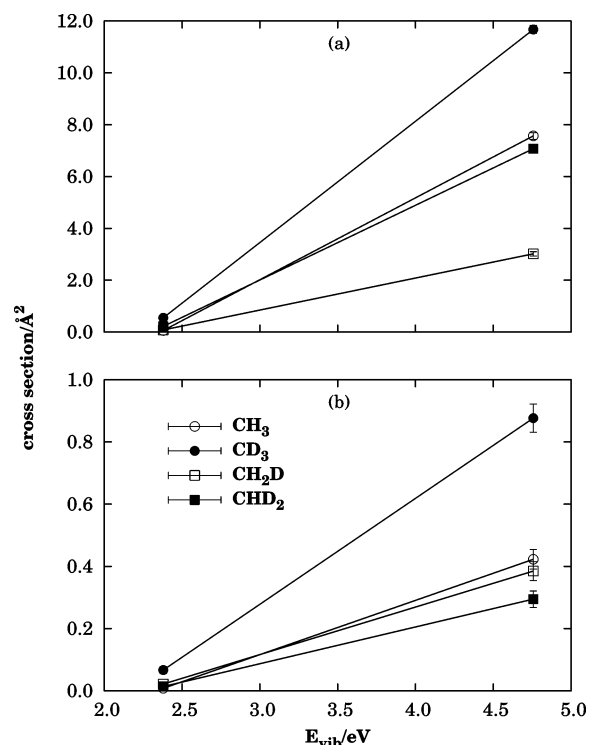*[a] Number of trajectories leading to formation of CH₂D₂ complexes that may dissociate to form either CH₂D or CHD₂ products with the corresponding ZPE. [b] N_d is the number of trajectories leading to direct formation of CH₂D; N_{RRKM} is the number of CH₂D₂ complexes predicted (by RRKM theory) to end to CH₂D with ZPE; σ_d is the direct-mechanism dissociative cross section for the formation of CH₂D, while $\Delta\sigma_d$ stems for the corresponding Monte Carlo standard deviation. [c] N_d is the number of trajectories leading to direct formation of CHD₂; N_{RRKM} is the number of CH₂D₂ complexes predicted (by RRKM theory) to end to CHD₂ with ZPE; σ_d is the direct-mechanism dissociative cross section for the formation of CHD₂, while $\Delta\sigma_d$ stems for the corresponding Monte Carlo standard deviation. [d] Total CID cross section (and the corresponding Monte Carlo standard deviation), including the contributions from both N_d (for the formation of CH₂D and CHD₂) and $N_{CH_2D_2^*}$ (see the text).*
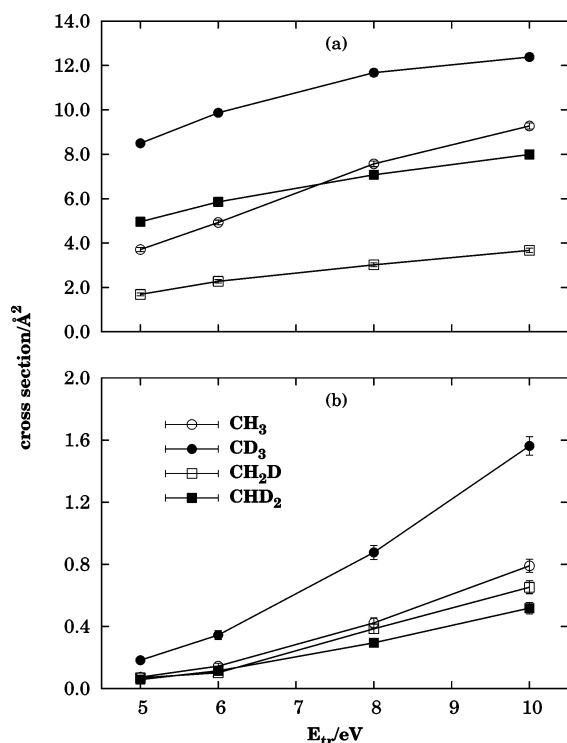
Figure 1. Collision-induced dissociation cross sections as a function of translational energy: (a) indirect dissociation; (b) direct dissociation. The error bars indicate the Monte Carlo standard deviation. See the text.

Figure 2. Collision-induced dissociation cross sections as a function of vibrational energy of the reactant molecule: (a) indirect dissociation; (b) direct dissociation. See the text.

$E_{ZPE}(CD_3)$ as displayed in Table 1. Also the difference in the energy transfer because of the collision with argon may have an influence on that result (this will be further detailed in the next subsection).

The effect of vibrational excitation on the indirect-type CID cross sections is addressed in Figures 2a and 3a. Note that the main trends of the curves in these figures are directly related to the numbers of complexes formed during the collision process, which are shown in Tables 2, 3, and 4 under the symbols $N_{CH_4^*}$, $N_{CD_4^*}$, and $N_{CH_2D_2^*}$, respectively. It is interesting to observe in Figure 2a that, for the three systems at $E_{tr} = 8$ eV, there is a great increase in the indirect CID process as the vibrational energy (E_{vib}) increases from 2.3785 eV to 4.757 eV; the factors are 126, 21, and 34 for Ar + CH₄, Ar + CD₄, and Ar + CH₂D₂, respectively. Furthermore, we note that Troya[26] has obtained almost negligible indirect-type CID cross sections by considering

hyperthermal argon collisions with vibrationally cold CH₄ molecules. Clearly, vibrational excitation has a strong impact in the enhancement of dissociation in methane and its isotopomers. Concerning the specific vibrational-mode excitation, one observes in Figure 3a that the indirect-type CID cross section slightly increases when most of the initial E_{vib} is placed in the high-frequency modes (symmetric and antisymmetric stretches).

Although the major contribution to the CID cross section arises from the indirect mechanism, direct-type trajectories may play an important role, especially as the energy (either collisional or internal) increases. We show in Figure 1b the CID cross sections arising from direct dissociation for fixed $E_{vib} = 4.757$ eV as a function of the collision energy. The contribution from direct mechanism to CID is not negligible even for $E_{tr} = 5$ eV, and increases with collision energy, as expected. Indeed, it is

Dissociation of the Ar + CH$_4$ Reaction

J. Phys. Chem. A, Vol. 110, No. 22, 2006 **7117**
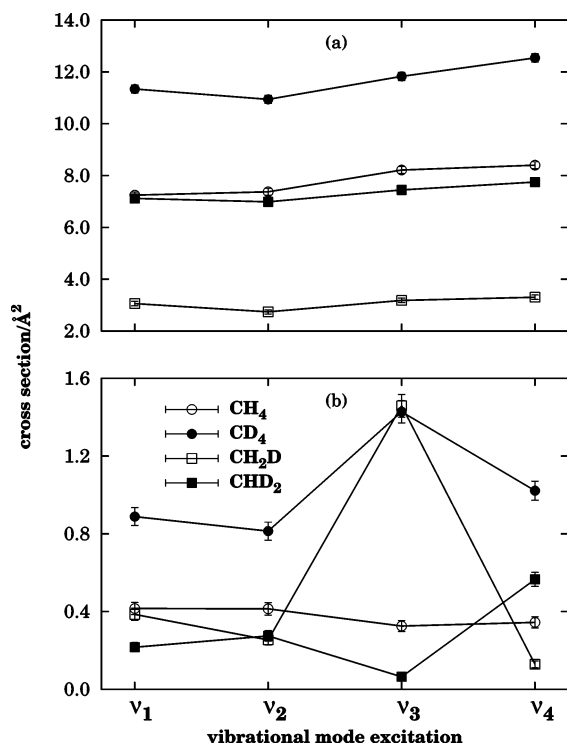
Figure 3. Collision-induced dissociation cross sections as a function of specific vibrational-mode excitation of the reactant molecule: (a) indirect dissociation; (b) direct dissociation. See the text.
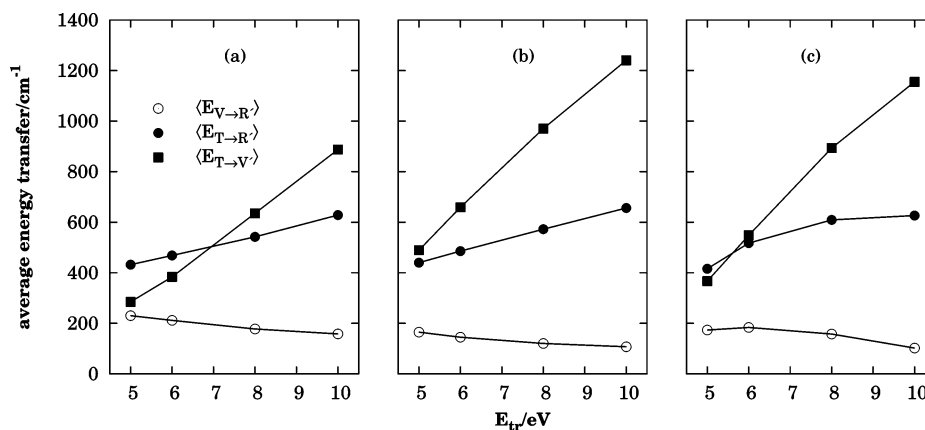

Figure 4. Energy transferred in all collisions as a function of translational energy for Ar + CH$_4$ (open circles), Ar + CD$_4$ (full circles), and Ar + CH$_2$D$_2$ (full squares).

of the same order of magnitude as the total CID cross section (essentially due to the contribution from indirect mechanism) calculated by Troya[26] for the collision of argon with a vibrationally cold CH$_4$ molecule at E_{tr} = 10 eV. Despite the differences between the intramolecular CH$_4$ potential used in both works, this discrepancy in the CID cross sections may be attributed to the vibrational excitation of methane, as it is discussed below. Figure 1b and Tables 2−4 also show that the direct-mechanism CID cross sections are always greater for Ar + CD$_4$ than for Ar + CH$_4$ and Ar + CH$_2$D$_2$; the CID cross sections increase by ∼11 and ∼9 as the collision energy increases from 5 eV to 10 eV, for Ar + CH$_4$ and the deuterated species, respectively. This result is in agreement with previous evidence[52] that the increase of the reduced mass leads to a better coupling between translational and vibrational degrees of freedom because of a decrease in the corresponding fundamental frequencies. Note also that, even for CID processes evolving on distinct potential energy surfaces (e.g., Ar + CH$_4$ and Ar + CF$_4$), the change in the mass of the system may account for most of the differences arising in the corresponding dynamics.[26] Another interesting observation in Figure 1b is the fact that the ratio of the cross sections for production of CH$_2$D and CHD$_2$ deviates from unity as the collision energy increases, favoring the formation of the latter species. This is in contrast with the above finding for indirect dissociation and can be rationalized by noting that the formation of CH$_2$D implies the cleavage of a C−D bond, which is more likely to happen than a cleavage of a C−H bond, as we have seen above in the comparison between Ar + CD$_4$ and Ar + CH$_4$ CID cross sections. In turn, the sum of both CH$_2$D and CHD$_2$ contributions to the direct-mechanism CID cross sections in the case of semideuteration stands between the corresponding values for CH$_4$ (the lowest) and CD$_4$ (the highest).
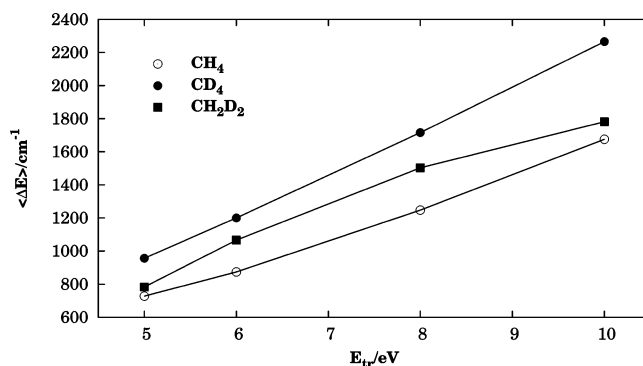
We represent in Figure 2b the direct-mechanism CID cross section for E_{tr} = 8 eV as a function of E_{vib}. It is apparent from this figure that vibrational excitation is important for direct dissociation to occur. This conclusion is particularly evident by the comparison of the present results with those of Troya,[26] who observed no direct-dissociative trajectories for the collision of Ar with CH$_4$ molecules prepared according to a thermal sampling of vibrational quantum numbers at T = 300 K (which essentially corresponds to the vibrational ground state), even for E_{tr} = 10 eV. In addition, Tables 2−4 show that direct-mechanism CID cross sections are enhanced by a factor of ∼53 (∼13) for Ar + CH$_4$ (Ar + CD$_4$) as the vibrational energy of reactants increases from 2.3785 eV to 4.757 eV, while the corresponding factor is 17.5 (21) for the formation of CH$_2$D (CHD$_2$) after the Ar + CH$_2$D$_2$ collision. We should emphasize that these enhancement factors are much larger than the corresponding ones reported above for the variation of collision energy. It is worth noting that the direct-mechanism CID cross sections for the deuterated species are always higher than the Ar + CH$_4$ ones, though the magnitude of the corresponding enhancement factors follows the reverse order. Combining the present result (including the above-mentioned for indirect dissociation) with the fact that methane-like species may be found in vibrational excited states at an orbital altitude,[34] we anticipate that degradation of polymeric hydrocarbons coating spacecrafts may be more significant than expected for vibrationally cold molecules.

Whether specific vibrational-mode excitation plays a significant role in direct-type dissociation is per se a very interesting question. To investigate this, we have performed trajectory calculations for specific excitations of each of the four types of vibrations (designated by ν_i, where i = 1−4), and plotted the results for the CID cross sections in Figure 3b. Because there is a partial redistribution of the vibrational energy localized in the excited mode during the time the colliding species are approaching each other, these results should be considered from a qualitative point of view. This well-known deficiency of the QCT method may contribute to attenuate the differences in the cross sections arising from each vibrational-mode excitation [as shown in Figure 3b], although the essential trends of the mode specificity can be still figured out and easily rationalized based on the atomic motion associated with the mode being excited (see below). As can be seen, for the deuterated species (both CD$_4$ and CH$_2$D$_2$), the symmetric stretch (ν_3) excitation is more likely to lead to direct CID than the excitation of other modes. This is not a surprising result because the symmetric stretch is expected to be the most coupled to the reaction path. In particular for Ar + CH$_2$D$_2$, the symmetric-stretch excitation clearly favors the formation of the CH$_2$D species (at the expense

Figure 5. Average values of the energy transferred in nondissociative trajectories for vibration to rotation ($\langle E_{V \to R'} \rangle$), translation to rotation ($\langle E_{T \to R'} \rangle$), and translation to vibration ($\langle E_{T \to V'} \rangle$) as a function of translational energy: (a) Ar + CH_4; (b) Ar + CD_4; (c) Ar + CH_2D_2.
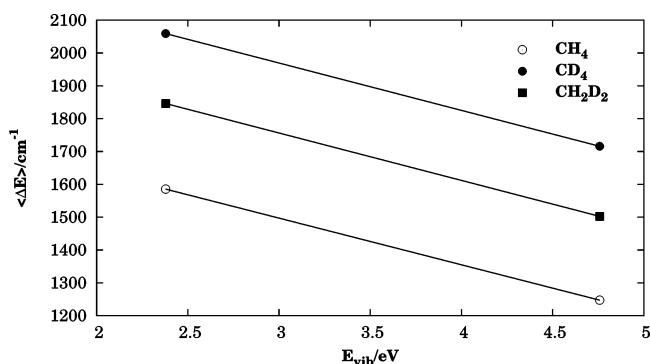
Figure 6. Energy transferred in all collisions as a function of vibrational energy for Ar + CH_4 (open circles), Ar + CD_4 (full circles), and Ar + CH_2D_2 (full squares).

of CHD_2) and the corresponding CID cross section coincides (within the error bars) with that for Ar + CD_4, which may be explained by the close values of the frequencies for the ν_3 mode in both CH_2D_2 and CD_4 (see Table 1). We should also stress that, in the case of CH_2D_2, the ν_3 mode corresponds essentially to the motion (in phase) of the deuterium atoms, which is better coupled with translation. In addition, unlike the ν_2 bending-modes excitation, for which the formation of CH_2D and CHD_2 is similar, the lowest-frequency modes (ν_1) excitation tends to favor CH_2D against CHD_2, while the reverse arises for the highest-frequency one (antisymmetric stretch). This can be explained based on the motions of the atoms associated to each mode in CH_2D_2. Thus, for the set of ν_4 modes, those associated

with frequencies 3185 and 3263 cm^{-1} are mainly characterized by the motion of the hydrogen atoms, while in the 2409 cm^{-1} mode the out-of-phase motion of deuterium atoms are prominent. In contrast, all the modes in the ν_1 set involve the motion of the deuterium atoms, but only two (1182 and 1343 cm^{-1}) are characterized by a significant motion of the hydrogens.
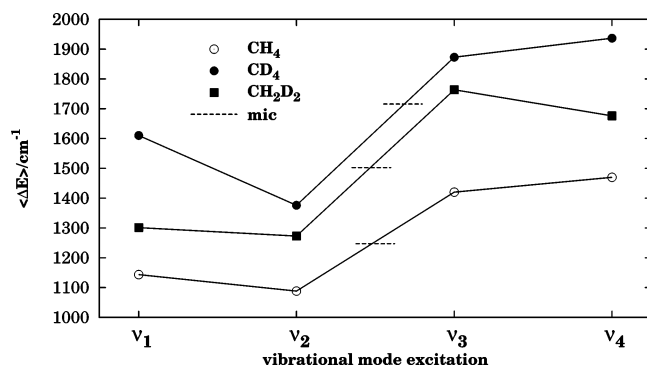
We recall here that vibrational-mode specificity has also been observed experimentally in the Cl + CH_2D_2 gas-phase reaction[53] as well as in the dissociation of CH_2D_2 on a nickel (100) surface.[54] The results of the present work for hyperthermal collisions of argon with CH_2D_2 constitute further evidence of such vibrational-mode specificity. This finding can be used to control the reaction outcome and provides clear evidence about the nonstatistical behavior of the CH_2D_2 dissociation. Hence, it may explain the opposite trends arising in the dissociation of CH_2D_2 via direct (where formation of CH_2D is generally favored) and indirect (where formation of CHD_2 is favored) mechanisms (see Figures 1−3 and Table 4).

Recently, both gas-phase[55] and gas−surface[56,57] experimental studies have shown that excitation of CH_4 stretch modes strongly enhances reactivity. Our results show that CID cross sections for Ar + CH_4 increase only slightly when the CH_4 stretch modes are excited. Although this quantitative discrepancy may be attributed to the fact that we are comparing different reactions, the apparent statistical behavior of methane in hyperthermal collisions with argon may be a consequence, to a certain extent, of partial deexcitation of the initially excited vibrational mode before the collision takes place, as pointed out above.

3.2. Energy Transfer. We plot in Figure 4 the average energy
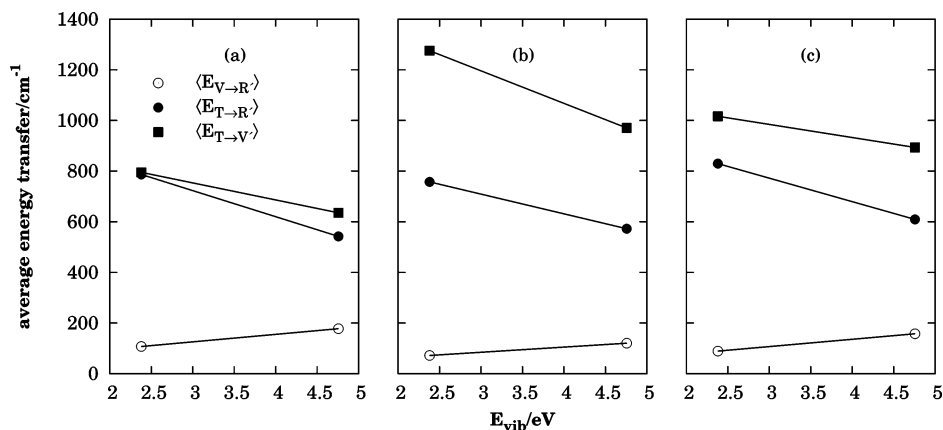
Figure 7. Average values of the energy transferred in nondissociative trajectories for vibration to rotation ($\langle E_{V \to R'} \rangle$), translation to rotation ($\langle E_{T \to R'} \rangle$), and translation to vibration ($\langle E_{T \to V'} \rangle$) as a function of vibrational energy: (a) Ar + CH_4; (b) Ar + CD_4; (c) Ar + CH_2D_2.

Dissociation of the Ar + CH$_4$ Reaction

*J. Phys. Chem. A, Vol. 110, No. 22, 2006* **7119**

Figure 8. Energy transferred in all collisions as a function of mode-specific excitation for Ar + CH$_4$ (open circles), Ar + CD$_4$ (full circles), and Ar + CH$_2$D$_2$ (full squares). The dashed lines indicate the corresponding microcanonical values.

transferred in all collisions as a function of collision energy (E_{tr}). It is clear from this figure that the energy transfer increases with E_{tr}, and it is always larger for Ar + CD$_4$, followed by Ar + CH$_2$D$_2$ and CH$_4$, respectively. This result follows the same trend that we have met in the previous subsection for the corresponding CID cross sections (especially for the indirect-type ones). The differences arising in the three systems may be justified by noting that the vibrational frequencies of CD$_4$ are lower than those for CH$_2$D$_2$ and CH$_4$ (see Table 1), which favors the T → V′ energy transfer in the former. This is confirmed in Figure 5 where we have plotted the average translational to vibrational ($\langle E_{T \to V'} \rangle$), translational to rotational ($\langle E_{T \to R'} \rangle$), and vibrational to rotational ($\langle E_{V \to R'} \rangle$) energy transfer for nondissociative trajectories as a function of collision energy. Indeed, it is apparent from this figure that $\langle E_{T \to V'} \rangle$ increases with collision energy and it is larger for the deuterated species (panels b and c) than for CH$_4$ (panel a). In addition, it is interesting to observe in Figure 5 that $\langle E_{T \to R'} \rangle$ also increases with collision energy, but at a smaller rate than $\langle E_{T \to V'} \rangle$, while $\langle E_{V \to R'} \rangle$ slightly decreases within the same range. This general trend does not change with the reactant system and, in particular, the values of $\langle E_{T \to R'} \rangle$ are approximately independent of the isotopomer considered. Thus, it is clear that T−R coupling, and mainly the V−R one, plays a minor role for the energy transfer mechanism in hyperthermal collisions of methane with argon when compared with T−V coupling. This is in contrast with our previous findings[25] for the same system at temperatures ranging from 2500 to 4500 K, where $\langle E_{T \to V'} \rangle$ and $\langle E_{T \to R'} \rangle$ were found to be much smaller than $\langle E_{V \to R'} \rangle$ (and the directions of the transfer of the average energies were reversed in relation to those in the present work). These differences may come from the

hyperthermal conditions where the high values of the collision energy produces hard collisions with large amounts of energy transferred to methane.

Figure 6 shows the average energy transferred in all collisions ($\langle \Delta E \rangle$) for E_{tr} = 8 eV as a function of vibrational energy. Once again, $\langle \Delta E \rangle$ is larger for Ar + CD$_4$, followed by Ar + CH$_2$D$_2$ and, finally, by Ar + CH$_4$. The increase of the vibrational energy of reactants leads to a decrease in $\langle \Delta E \rangle$, which must be due to a less efficient T−V and T−R coupling. This observation implies that it is more difficult to vibrationally excite methane and its deuterated isotopomers by collision with argon when they are already excited; hence, this kind of collision may contribute to the excitation of methane-like molecules in LEO, with obvious consequences to their reactivity (see previous subsection). Furthermore, it is interesting to note in Figure 7 that, for all the reactant systems, the fluxes of energy for nondissociative trajectories as a function of the vibrational energy show the opposite trend of that discussed above for the corresponding variation with increasing collision energy (Figure 5): $\langle E_{T \to V'} \rangle$ and $\langle E_{T \to R'} \rangle$ decrease with increasing vibrational energy, while $\langle E_{V \to R'} \rangle$ slightly increases. Thus, the energy transfer between translation and internal degrees of freedom is favored with increasing collision energy rather than with vibrational excitation, while the reverse is true for $\langle E_{V \to R'} \rangle$.

Figure 8 displays the average energy transferred in all collisions for E_{tr} = 8 eV as a function of specific vibrational-mode excitation. It is shown in this figure that the average energy transfer is promoted by exciting the high-frequency modes (i.e., symmetric and antisymmetric stretches), while the excitation of the low-frequency ones (i.e., bending-type) does not favor it in relation to the corresponding microcanonical vibration distribution (dashed lines in the figure). Moreover, it is shown in Figure 9 that, for all the three systems, T → V′ and T → R′ energy transfer occurs preferentially in the case of exciting the symmetric- and antisymmetric-stretching modes, while the excitation of lower-frequency modes (ν_1 and ν_2) leads to values of $\langle E_{T \to V'} \rangle$ and $\langle E_{T \to R'} \rangle$ slightly below the corresponding ones for the microcanonical vibrational distribution (see also Figure 5). This may be attributed to the fact that large-amplitude vibrational stretches should couple better with translation than excited low-frequency (bending-type) vibrations. Indeed, exciting high-frequency modes brings the system to a situation where the corresponding vibrational states are more closely spaced (i.e., the system becomes more anharmonic than in the ground vibrational state), which allows a more efficient T−V coupling; such a statement has been already applied in a previous energy transfer study[20] of thermal collisions (500 ≤ T/K ≤ 5000) of
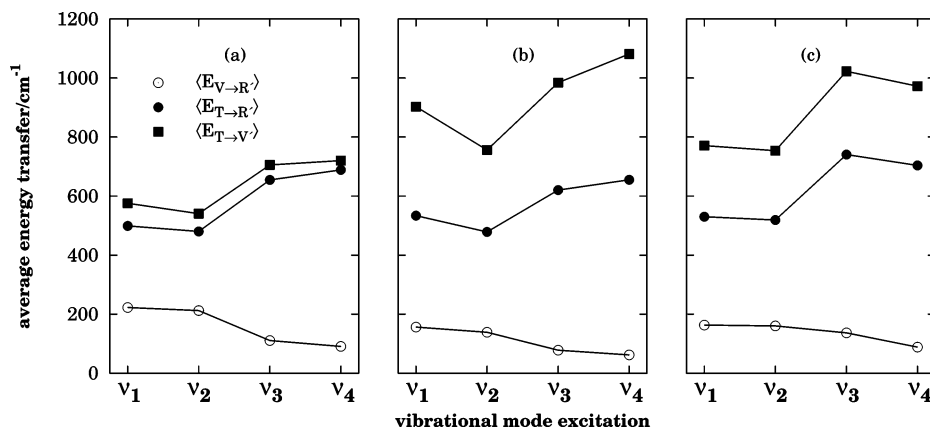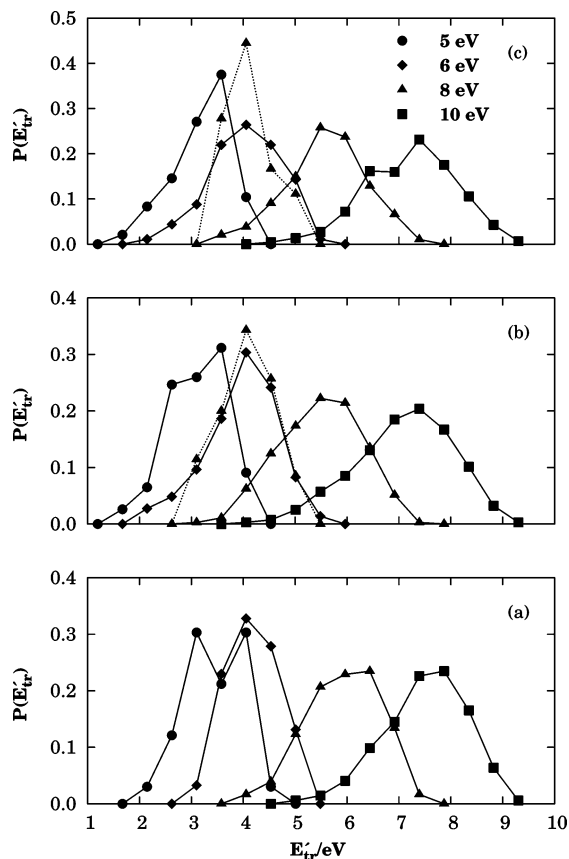

Figure 9. Average values of the energy transferred in nondissociative trajectories for vibration to rotation ($\langle E_{V \to R'} \rangle$), translation to rotation ($\langle E_{T \to R'} \rangle$), and translation to vibration ($\langle E_{T \to V'} \rangle$) as a function of mode-specific excitation: (a) Ar + CH$_4$; (b) Ar + CD$_4$; (c) Ar + CH$_2$D$_2$.
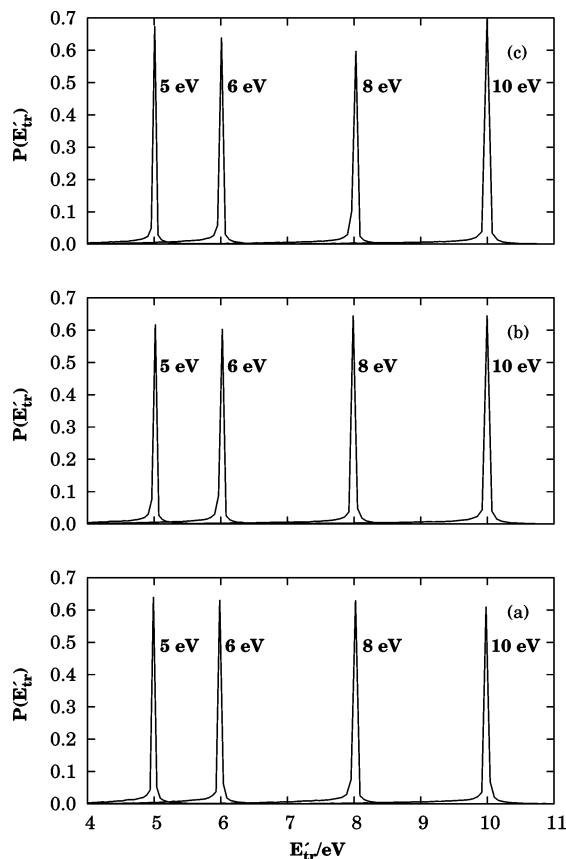
Figure 10. Final translational energy distribution for nondissociative trajectories at E_{tr} = 5, 6, 8, and 10 eV (E_{vib} = 4.757 eV): (a) Ar + CH$_4$; (b) Ar + CD$_4$; (c) Ar + CH$_2$D$_2$.

Figure 11. Final translational energy distribution for dissociative trajectories at E_{tr} = 5, 6, 8, and 10 eV: (a) Ar + CH$_4$; (b) Ar + CD$_4$; (c) Ar + CH$_2$D$_2$. In panels b and c, the distributions for E_{tr} = 8 eV at both E_{vib} = 2.3785 eV (dashed line) and E_{vib} = 4.757 eV (solid line) are shown; the former is not represented in panel a, because only four trajectories lead to direct dissociation.

argon with highly excited tetrahedral molecules (i.e., CH$_4$, CD$_4$, SiH$_4$, and CF$_4$). In contrast, excitation of modes ν_3 and ν_4 causes $\langle E_{V \to R} \rangle$ to diminish in relation to the excitation of modes ν_1 and ν_2, which may be associated to the fact that bending-type vibrations are expected to be more coupled with rotational motion.

We represent in Figure 10 the translational energy distribution for nondissociative trajectories at E_{tr} = 5, 6, 8, and 10 eV (E_{vib} = 4.757 eV). The distributions for the remaining calculations at E_{tr} = 8 eV (not shown in the figure) present a very similar pattern. It is clear from this figure that, for the three systems, the peak of each distribution is placed around the corresponding initial collision energy, which indicates that most of the trajectories transfer very little energy. A similar result has been obtained by Troya[26] for hyperthermal collisions between argon and vibrationally cold CH$_4$ molecules. In fact, the average energy transferred from translation to the internal degrees of freedom appears to be controlled by the great amount of energy transferred with small probability (left-hand tail of the curves in Figure 10). However, the distributions in this figure exclude all trajectories leading to direct dissociation, in which a great amount of collision energy must be transferred into the internal degrees of freedom of the reactant molecule. Then, we present in Figure 11 the translational energy distributions for direct-type dissociative trajectories at E_{tr} = 5, 6, 8, and 10 eV (E_{vib} = 4.757 eV). For Ar + CD$_4$ and Ar + CH$_2$D$_2$ at E_{tr} = 8 eV, the distributions for E_{vib} = 2.3785 eV are also represented by dashed lines. It is clear from this figure that the maxima of distributions are always shifted to lower collision energies (in relation to the corresponding value of E_{tr}): they vary from ~1.5 (~1.4) to ~2.1 eV (~2.6 eV) in the case of Ar + CH$_4$ (Ar + CD$_4$ and Ar + CH$_2$D$_2$). This expected result shows that most of the direct-

type dissociative trajectories transfer more than 1.4 eV to the internal degrees of freedom of the reactant molecule; these shifts are even enhanced to ~3.9 eV in the case of E_{vib} = 2.3785 eV (for Ar + CD$_4$ and Ar + CH$_2$D$_2$), which confirms the above observation that energy transfer decreases with vibrational excitation. Note also that the distributions broaden for the deuterated species which appears to reflect the increase in the number of internal states available.

4. Conclusions

We have applied the quasi-classical trajectory method to study the effect of vibrational energy excitation of methane in the collision-induced dissociation by argon at hyperthermal energies ($5 \leq E_{tr}/eV \leq 10$). Trajectory calculations have been also carried out for Ar + CD$_4$ and Ar + CH$_2$D$_2$ in order to assess the importance of isotope substitution on the title reaction. In all cases, we have used a recently modified version[25] of the CH$_4$ potential energy surface of Duchovic et al.,[43] while the Ar–CH$_4$ interactions have been modeled by the pairwise generalized exponential function of Troya.[26]

Although the major contribution to CID may arise from long-lived complexes (indirect mechanism), the importance of direct-type trajectories is not negligible, especially as either collision energy or vibrational energy increases. The direct-mechanism CID cross sections follow the order σ_{CID}(Ar + CD$_4$) > σ_{CID}(Ar + CH$_2$D$_2$) > σ_{CID}(Ar + CH$_4$), which has been attributed to a better T–V coupling as deuteration increases owing to a decrease of the corresponding fundamental vibrational frequencies. On the other hand, the differences arising in the indirect-

Dissociation of the Ar + CH$_4$ Reaction

J. Phys. Chem. A, Vol. 110, No. 22, 2006 **7121**

mechanism CID cross sections for the three systems have been explained on the basis of the ZPEs of the forming products.

From the calculations with mode-specific excitation conditions, we found that direct dissociation of CH$_4$ is essentially independent of the mode where the energy is pooled, while CD$_4$ and CH$_2$D$_2$ present mode specificity (CID is enhanced for symmetric- and antisymmetric-stretches excitation). This mode specificity has implications for the control of the reactions and prevents the application of statistical theories to these systems. However, the energy transfer in Ar + CH$_4$ (as well as in Ar + CD$_4$ and Ar + CH$_2$D$_2$) is enhanced by exciting the stretch vibrational modes of the colliding molecule.

For energy transfer, we have observed that most of the nondissociative events led to little energy transfer from translational to internal degrees of freedom, being the values of $\langle E_{T \to V} \rangle$ and $\langle E_{T \to R} \rangle$ essentially controlled by the great amount of energy transferred with small probability. In contrast, most of direct-type dissociative trajectories involve a great amount of energy transfer into internal degrees of freedom (more than 1.4 eV) for all the three systems studied in this work.

Finally, the present results clearly point out the strong impact of vibrational excitation on the collision-induced dissociation of methane-like molecules at LEO hyperthermal conditions. Since such molecules (that can be seen as building blocks for hydrocarbon polymers, e.g., polyethylene) may appear vibrationally excited at orbital altitude,[34] one anticipates this factor to constitute an additional contribution to the faster degradation of the spacecraft's polymeric coat under LEO conditions. Moreover, energy transfer is significant for low vibrational energies, which may be a pumping source of collision energy into internal energy, and hence excite the CH$_4$ molecules that can more easily dissociate after colliding again with argon or other species.

References and Notes

(1) Oref, I.; Tardy, D. C. *Chem. Rev.* **1990**, *90*, 1407.
(2) Hippler, H.; Troe, J. *Bimolecular Collisions*; Baggot, J. E., Ashfold, M. N. R., Eds.; The Royal Society of Chemistry: London, 1989; p 209.
(3) Mayne, H. R. *Int. Rev. Phys. Chem.* **1991**, *10*, 107.
(4) Rodrigues, S. P. J.; Varandas, A. J. C. *J. Phys. Chem. A* **1998**, *102*, 6266.
(5) Martin, P. G.; Keogh, W. J.; Mandy, M. E. *AstroPhys. J.* **1998**, *499*, 793.
(6) Ceballos, A.; Garcia, E.; Laganà, A. *J. Phys. Chem. Ref. Data* **2002**, *31*, 371.
(7) Brown, N. J.; Miller, J. A. *J. Chem. Phys.* **1984**, *80*, 5568.
(8) Lendvay, G.; Schatz, G. C. *Classical Trajectory Methods for Studying Energy Transfer from Highly Vibrationally Excited Molecules;* Barker, R. J., Ed.; JAI Press: Greenwich, CT, 1995; Vol. 2.B, p 481.
(9) Kleiman, J. I.; Iskanderova, Z. A.; Pérez, F. J.; Tennyson, R. C. *Surf. Coat. Technol.* **1995**, *76*, 827.
(10) Minton, T. K.; Garton, D. J. *Advances Series in Physical Chemistry*; Dressler, R. A., Ed.; World Scientific: Singapore, 2001; Vol. 11, p 420.
(11) Garton, D. J.; Minton, T. K.; Troya, D.; Pascual, R.; Schatz, G. C. *J. Phys. Chem. A* **2003**, *107*, 4583.
(12) Troya, D.; Schatz, G. C. *Int. Rev. Phys. Chem.* **2004**, *23*, 341.

(13) Troya, D.; Schatz, G. C. *Theory of Chemical Reaction Dynamics*; Laganà, A., Lendvay, G., Eds.; Kluwer Academic Publishers: Dordrecht, The Netherlands, 2004; p 329.
(14) Minton, T. K.; Zhang, J.; Garton, D. J.; Seale, J. W. *High Perform. Polym.* **2000**, *12*, 27.
(15) Zhang, J.; Minton, T. K. *High Perform. Polym.* **2000**, *13*, 467.
(16) Brunsvold, A. L.; Garton, D. J.; Minton, T. K.; Troya, D.; Schatz, G. C. *J. Chem. Phys.* **2004**, *121*, 11702.
(17) Lee, Y. T.; McDonald, J. D.; LeBreton, P. R.; Herschbach, D. R. *Rev. Sci. Instrum.* **1969**, *40*, 1402.
(18) O'Laughlin, M. J.; Reid, B. P.; Sparks, R. K. *J. Chem. Phys.* **1985**, *83*, 5643.
(19) Zhang, J.; Garton, D. J.; Minton, T. K. *J. Chem. Phys.* **2002**, *117*, 2746.
(20) Grinchak, M. B.; Levitsky, A. A.; Polak, L. S.; Umanskii, S. Y. *Chem. Phys.* **1984**, *88*, 365.
(21) Hase, W. L.; Date, N.; Bhuiyan, L. B.; Buckowski, D. G. *J. Phys. Chem.* **1985**, *89*, 2502.
(22) Hu, X.; Hase, W. L. *J. Phys. Chem.* **1988**, *92*, 4040.
(23) Cobos, C. J.; Troe, J. *Z. Phys. Chem. Neue Folge* **1990**, *167*, 129.
(24) Miller, J. A.; Klippenstein, S. J.; Raffy, C. *J. Phys. Chem. A* **2002**, *106*, 4904.
(25) Marques, J. M. C.; Martínez-Núñez, E.; Fernández-Ramos, A.; Vázquez, S. A. *J. Phys. Chem. A* **2005**, *109*, 5415.
(26) Troya, D. *J. Phys. Chem. A* **2005**, *109*, 5814.
(27) Roth, P.; Just, T. *Ber. Bunsen-Ges. Phys. Chem.* **1975**, *79*, 682.
(28) Tabayashi, K.; Bauer, S. H. *Combust. Flame* **1979**, *34*, 63.
(29) Klemm, R. B.; Sutherland, J. W.; Rabinowitz, M. J.; Patterson, P. M.; Quartemont, J. M.; Tao, W. *J. Phys. Chem.* **1992**, *96*, 1786.
(30) Kiefer, J. H.; Kumaran, S. S. *J. Phys. Chem.* **1993**, *97*, 414.
(31) Davidson, D. F.; Hanson, R. K.; Bowman, C. T. *Int. J. Chem. Kinet.* **1995**, *27*, 305.
(32) Koike, T.; Kudo, M.; Maeda, I.; Yamada, H. *Int. J. Chem. Kinet.* **2000**, *32*, 1.
(33) Warnatz, J. *Combustion Chemistry*; Gardiner, W. C. J., Ed.; Springer-Verlag: New York, 1984; p 197.
(34) Zhou, D. K.; Pendleton, W. R., Jr.; Bingham, G. E.; Thompson, D. C.; Raitt, W. J.; Nadile, R. M. *J. Geophys. Res.* **1994**, *99*, 19585.
(35) Varandas, A. J. C.; Zhang, L. *Chem. Phys. Lett.* **2001**, *340*, 62.
(36) Varandas, A. J. C. *ChemPhysChem* **2002**, *3*, 433.
(37) Garrido, J. D.; Caridade, P. J. S. B.; Varandas, A. J. C. *J. Phys. Chem. A* **2002**, *106*, 5314.
(38) Varandas, A. J. C. *J. Phys. Chem. A* **2003**, *107*, 3769.
(39) Varandas, A. J. C. *J. Phys. Chem. A* **2004**, *108*, 758.
(40) Teixeira, O. B. M.; Marques, J. M. C.; Varandas, A. J. C. *Phys. Chem. Chem. Phys.* **2004**, *6*, 2179.
(41) Varandas, A. J. C. *ChemPhysChem* **2005**, *6*, 453.
(42) Meinel, A. B. *Astrophys. J.* **1950**, *111*, 555.
(43) Duchovic, R. J.; Hase, W. L.; Schlegel, H. B. *J. Phys. Chem.* **1984**, *88*, 1339.
(44) Sun, L.; Claire, P. S.; Meroueh, O.; Hase, W. L. *J. Chem. Phys.* **2001**, *114*, 535.
(45) Varandas, A. J. C.; Pais, A. A. C. C.; Marques, J. M. C.; Wang, W. *Chem. Phys. Lett.* **1996**, *249*, 264.
(46) Marques, J. M. C.; Wang, W.; Pais, A. A. C. C.; Varandas, A. J. C. *J. Phys. Chem.* **1996**, *100*, 17513.
(47) Marques, J. M. C.; Varandas, A. J. C. *J. Phys. Chem.* **1997**, *101*, 5168.
(48) Hase, W. L. *MERCURY: A General Monte Carlo Classical Trajectory Computer Program;* Wayne State University: Detroit, MI.
(49) Lim, K. F.; Gilbert, R. G. *J. Phys. Chem.* **1990**, *94*, 72.
(50) Hase, W. L.; Buckowski, D. G. *Chem. Phys. Lett.* **1980**, *74*, 284.
(51) Dennison, D. M. *Rev. Mod. Phys.* **1940**, *12*, 175.
(52) Lenzer, T.; Luther, K.; Troe, J.; Gilbert, R. G.; Lim, K. F. *J. Chem. Phys.* **1995**, *103*, 626.
(53) Bechtel, H. A.; Kim, Z. H.; Camden, J. P.; Zare, R. N. *J. Chem. Phys.* **2004**, *120*, 791.
(54) Beck, R. D.; Maroni, P.; Papageorgopoulos, D. C.; Dang, T. T.; Schmid, M. P.; Rizzo, T. R. *Science* **2003**, *302*, 98.
(55) Camden, J. P.; Bechtel, H. A.; Brown, D. J. A.; Zare, R. N. *J. Chem. Phys.* **2005**, *123*, 134301.
(56) Maroni, P.; Papageorgopoulos, D. C.; Sacchi, M.; Dang, T. T.; Beck, R. D.; Rizzo, T. R. *Phys. Rev. Lett.* **2005**, *94*, 246104.
(57) Juurlink, L. B. F.; Smith, R. R.; Killelea, D. R.; Utz, A. L. *Phys. Rev. Lett.* **2005**, *94*, 208303.